Heliyon 10 (2024) e29892

Contents lists available at ScienceDirect

Heliyon

journal homepage: www.cell.com/heliyon

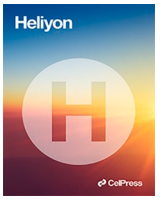

Research article

Improvement of mechanical performance on zirconium dioxide nanoparticle synthesized magnesium alloy nano composite

R. Venkatesh [a], M. Vignesh Kumar [b], I. Kantharaj [c], Roshita David [c], Melvin Victor De Poures [a], Ismail Hossain [d], A.H. Seikh [e], M.A. Kalam [f], Murugan P [g,*]

[a] Department of Mechanical Engineering, Saveetha School of Engineering, Saveetha Institute of Medical and Technical Sciences (SIMATS), Saveetha University, Chennai, 602105, Tamilnadu, India
[b] Department of Mechanical Engineering, KCG College of Technology, Karapakkam, Chennai, Tamil Nadu, 600097, India
[c] Department of Mechanical Engineering, Faculty of Engineering and Technology, Jain University, Bengaluru, Karnataka, 560069, India
[d] Department of Nuclear and Renewable Energy, Ural Federal University, Yekaterinburg, 620002, Russia
[e] Mechanical Engineering Department, College of Engineering, King Saud University, Riyadh, 11421, Saudi Arabia
[f] School of Civil and Environmental Engineering, FEIT, University of Technology, Sydney, Ultimo, NSW, Australia
[g] Department of Mechanical Engineering, Jimma Institute of Technology, JIMMA University, Ethiopia

ARTICLE INFO

Keywords:
AZ31B alloy
Inert-argon nature
Stir casting
Characteristics

ABSTRACT

With excellent mechanical properties and distinct solidification, the AZ31B series magnesium alloy has great potential for targeting engineering applications and synthesized via die casting process found a drawback on oxidation results porosity and reduced mechanical properties. Here, the magnesium alloy AZ31B series nanocomposite was synthesized with varied weight percentages of zirconium dioxide nanoparticles through a liquid metallurgy route with an applied stir speed of 200 rpm under an argon nature. With the help of a scanning electron microscope, the distribution of particles in the composite surface was found to be homogenous and void-free surface, which output results in less percentage of porosity (<1 %), and the composite contained 6 wt% ZrO_2 offers superior yield strength (212 ± 3 MPa), tensile strength (278 ± 2 MPa), and impact strength of 16.4 ± 0.4 J/mm^2. In addition, 8 wt% ZrO_2 blended composite showed the maximum microhardness value (78.3 ± 1 HV). The best-enhanced result of NC3 (AZ31B/6 wt% ZrO_2) is suggested for lightweight to high-strength structural applications.

1. Introduction

Nanocomposite materials were a significant choice for replacing conventional materials due to their unique characteristics, including good mechanical, wear, and thermal behaviour [1–3]. Due to the weight reduction, the automotive industries focused on magnesium alloy nanocomposite [4,5]. In past decades, aluminium alloy composite was used in automotive and aerospace applications due to its high ductility and good strength [6–8]. The magnesium-based alloy was found to have a 36 % reduction in weight compared with aluminium materials [9,10]. Its characteristics were enhanced by the additions of organic (fly ash), inorganic (ceramic particles), and fiber-based reinforcements [11–13]. Generally, solid state [14,15], liquid state [16–18], and vapour state processing [19].

* Corresponding author.
E-mail address: murugan.ponnusamy@ju.edu.et (M. P).

https://doi.org/10.1016/j.heliyon.2024.e29892
Received 23 March 2023; Received in revised form 16 April 2024; Accepted 17 April 2024
Available online 21 April 2024

Due to the economical, efficient, and simple process, liquid metallurgy (stir cast) was referred to Refs. [20–23]. The wear behaviour of TiC particles blended magnesium alloy (AZ31) composite was processed via stir cast route under ultrasonic nature. The output results of the tested composite with higher content of TiC proved high wear resistance compared to conventional cast AZ31alloy [24]. Most recently, Kumar et al. [25] prepared and studied the microstructural and mechanical performance of aluminium alloy composite blended with zirconium dioxide nanoparticles via stir casting. They reported that the composite contained 6 wt% of ZrO_2 and recorded a maximum tensile strength of 174.9 MPa, and compared to cast alloy, it was hiked by 44 %. In addition, the cryogenic treatment was one of the surface modification processes. It resulted in increased mechanical strength of the material [26]. The effect of ceramic particles on the microstructural and mechanical behaviour of mechanical stir cast developed AZ61 alloy composite and reported that the uniform stir speed leads to uniform particle distribution, which results in good mechanical properties of composite [27]. Stir cast fabricated AZ31/SiC composite microstructural, fractography and mechanical behaviour were studied. The surface morphology proved the presence of SiC as a homogenous distribution in the AZ31 matrix. The results showed that 4 % SiC facilitated maximum compression strength and hardness value compared to cast AZ31 alloy [28].

In addition, magnesium alloy composite's characteristics varied due to the casting process parameters, reinforcement percentage, and geometric shape. Generally, the magnesium matrix composites were developed with alumina, graphite, titanium carbide and carbon nanotube through the stir cast process. They found good wettability results in increased particle distribution with good interfacial bond strength reported by Sheikh et al. [29]. Several research articles addressed the optimum stir-casting process parameter for obtaining the porosity-free homogenous structure composite [30]. As reported, 700 °C melting temperature with 200 rpm stir speed developed magnesium alloy composite with uniform particle distribution makes a homogenous structure with the highest tensile strength [31,32]. The AZ91D alloy composite was synthesized using different mass fractions of nanoglass particles through stir casting. The effect of glass particles on microstructural and mechanical properties was measured experimentally and reported that the composite has better mechanical performance.

Recently, Thakur et al. [33] experimentally evaluated the mechanical properties of AZ31B/alumina for biomedical applications. The 0.5 % alumina nanoparticles and 0.3 % hydroxyapatite showed the highest compression strength, hardness, and corrosion resistance. Based on the various literature related to magnesium alloy composite process selection, reinforcement significance in magnesium alloy, limitations, and enhancement of mechanical and wear properties were discussed. The problem on conventional stir cast was porosity/void formation due to oxide formation. Due to this, the research attempts to synthesize the magnesium alloy (AZ31B) nanocomposite developed with ZrO_2 under argon nature via stir cast route and evaluated the influences of argon atmosphere on AZ31B alloy nanocomposite with ZrO_2 behaviour was experimentally studied. The composite containing 6 wt% ZrO_2 offers the highest yield strength, tensile strength and impact toughness compared to cast AZ31B alloy. The optimum result of the NC3 sample (AZ31B/6 wt% ZrO_2) is suggested for lightweight to high-strength structural applications.

2. Material and methods

2.1. Details for matrix and reinforcement materials

The magnesium alloy (AZ31) was selected as a matrix base due to its significant mechanical properties, good solubility, and good machinability [34–36]. Table 1 shows the constitution weight percentage details for AZ31B.

The 50-nm zirconium dioxide (ZrO_2) was considered a reinforcement particle adapted to AZ31B alloy by stir casting route. The ZrO_2 has good resistance against corrosion, high hardness and heat resistance, and high strength and durability [37]. In addition, Table 2 shows the physic-mechanical behaviour of AZ31B & ZrO_2 [38,39].

2.2. Preparation of magnesium alloy nanocomposites

Here, the preparation of magnesium alloy with and without ZrO_2 was followed by (weight ratios) Table 3 and its fabrication technical details are addressed in Table 4. Accordingly, a digital balancing machine weighted the AZ31B alloy ingots and ZrO2 nanoparticles. After the AZ31B alloy ingots were placed in a graphite crucible, as shown in Fig.1and, the ZrO_2 was kept in a muffle furnace at 300 °C for 30 min. The graphite crucible was placed over the electrical furnace setup, and the magnesium alloy was preheated at 600 °C for 10 min. A thermocouple monitored the temperature of the furnace. The initial preheating process helps to remove the moisture content [4,5].

Then, the temperature of the furnace was increased to 700 °C for 10 min under argon nature, which helps to limit the oxidation [17,18]. During this process, the AZ31B alloy was fully melted like a liquid stage, and its temperature was reduced to 550 °C like a semisolid stage to add the externally preheated ZrO_2 nanoparticles. Finally, the AZ31B alloy and ZrO_2 were mixed via mechanical stir action of 200 rpm for 20 min, which helped to uniform particle distribution reported by Hanizam et al. [31]. Finally, the mixed molten metal was poured into a preheated (300 °C) tool steel rectangular (150 mm × 50 mm x 20 mm) die and cured by natural convection.

Table 1
Chemical composition of Z31B series magnesium alloy.

Constitutions	Al	Fe	Si	Mn	Zn	Mg
wt%	2.92	0.005	0.1	0.3	1.09	95.58

Table 2
Physio-mechanical properties of AZ31B and ZrO_2.

Material/Properties	Density	Ultimate tensile strength	Yield strength	Hardness	Thermal conductivity	Melting point
	g/cc	MPa	MPa	VHN	W/mK	°C
AZ31B	1.77	260	200	66	84	605–630
ZrO_2	5.89	–	–	1300	1.675	2681–2847

Table 3
Weight percentages of AZ31B and ZrO_2 nanoparticles.

Composite Identification	Weight of matrix and reinforcement in wt%	
	Magnesium alloy (AZ31B)	Zirconium dioxide (ZrO_2)
Cast AZ31B	100	0
NC1	98	2
NC2	96	4
NC3	94	6
NC4	92	8

Table 4
Technical descriptions for composite preparation.

S.No	Technical descriptions	Unit and dimensions
1	Crucible capacity	5 kg
2	Furnace operating temperature	100 to 1000 °C
3	Preheating temperature (AZ31B)	600 °C
4	Melting temperature (AZ31B)	700 °C
5	Semisolid state temperature (AZ31B)	550 °C
6	Medium of inert gas	Argon
7	Type of stirrer	Twin blade-SS
8	Speed of stirrer	200 rpm
9	Time to stirrer	20 min
10	ZrO_2 preheating temperature	300 °C
11	Die preheating temperature	300 °C
12	Size of Die	150 mm × 50 mm X 20 mm

2.3. Technical details for testing of developed composites (Characterization study)

The concept of Archimedes & rule of mixture measured the actual and theoretical density of developed composites. High-Tech make ZEISS model SEM was utilized to examine the surface morphology of cast AZ31B alloy and its nanocomposite prepared with

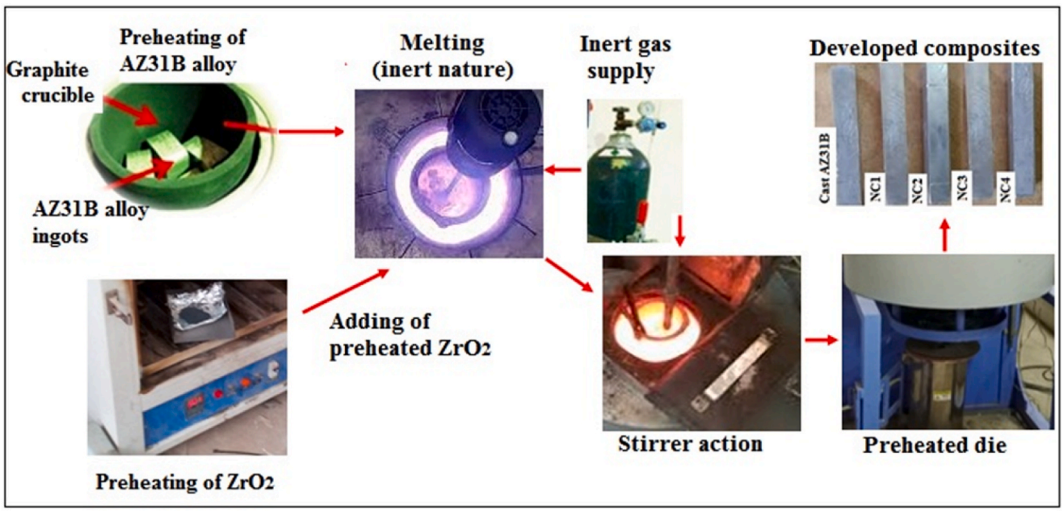

Fig. 1. Flow process layout for AZ31B alloy and its nanocomposite preparations.

ZrO_2 nanoparticles. The composite samples were cut as 10 mm × 10 mm ×10 mm cubic surfaces polished via various emery grades and glass polish made with a mechanical rotating polishing machine [4,5].

FIE make UT40 model 40-ton capacity universal testing machine was used to evaluate the tensile performance of the developed AZ31 alloy and its nanocomposites with 5 mm/min cross slide speed. The ASTM E08 standard (104 mm × 10 mm x 6 mm) was followed [17]. FIE-made VM50 model, microhardness tester, was involved in hardness evaluation. ASTM E92 standard (50 mm × 10 mm x 10 mm) prepared sample was tested by 100 g load for 10 s with diamond tip indenter. The Charpy impact test machine made by FIE of the IT30 model was utilized to estimate composite impact strength, followed by ASTM E23 (55 mm × 10 mm x 10 mm). In mechanical evaluation, three tests were conducted from each composite, and an average of three was taken as the final value (see Fig. 1).

3. Results and discussions

3.1. Density (actual and theoretical) and porosity percentage

Here, the (actual/theoretical) density and percentage of porosity of cast magnesium alloy (AZ31B) and NC1, NC2, NC3, and N4 are shown in Fig. 2. With compared to theoretical density, the actual density of fabricated composite was low due to voids and micro-porosity [4]. The actual density of AZ31B cast alloy was 1.75 g/cc. At the same time, the additions of 2 wt% ZrO_2 were recorded as 1.7 6 g/cc. It was due to the effect of a blended mixture that obeys the rule of mixture [10,11]. Further inclusions of ZrO_2 as 4, 6, and 8 wt% in AZ31B matrix noted by progressive improvement and composite containing maximum weight percentages of ZrO_2 proved their least weight gain as 4 % compared to cast AZ31B alloy.

However, the porosity of cast magnesium alloy (AZ31) was identified by 1.13 %, and the additions of ZrO_2 for 2, 4, 6, and 8 wt% showed a marginal downtrend and varied from 1.12 % to 1.09 %, respectively. The variation in the porosity of the composite was due to thermal mismatch during the fabrication of the composite [13,16]. In previous research, the composite was fabricated by stir cast process with applied vacuum pressure to limit the casting defects [18]. At the same time, the porosity of developed composites didn't exceed 2 % due to the uniform stir speed of 200 rpm for 20 min. More than 5 % of porosity changes to structural failure and low mechanical behaviour [31].

3.2. Surface morphology studies

The scanning electron microscope recorded surface morphology of magnesium alloy (AZ31B) nanocomposites prepared with 0, 2, 4, 6, and 8 wt% is shown in Fig. 3(a–e). These images proved the presence of ZrO_2 nanoparticles in the AZ31B matrix. The slag-free fine grain microstructure with little micro-porosity was noted by cast AZ31B alloy and illustrated in Fig. 3 (a). The thermal mismatch was the reason for the microporosity reported by Baraniraj et al. [4].

Fig. 3(b) indicates the surface morphology of AZ31B alloy nanocomposite developed with 2 wt% ZrO_2 (NC1). The presence of ZrO_2 was identified as a white dot field, and its identification was detailed in Fig. 3(b). However, the particle was strongly dispersed in the AZ31B alloy matrix and made uniform particle distribution due to the applied uniform stir speed of 200 rpm for 20 min. Previous research [18] reported that the uniform stir action leads to homogenous particle distribution, increasing composite tensile strength.

THE AZ31B alloy nanocomposite prepared with 4 wt% ZrO_2 nanoparticle is represented in Fig. 3(c). The white dot indication of ZrO_2 in the AZ31B alloy matrix is uniform and distributed throughout the matrix, increasing the tensile strength of the composite. Earlier, Ratna Sunil et al. [14] obtained homogenous particle distribution due to the applied uniform stir speed under a semisolid state of molten metal. In addition, the agglomerate particle formation in the base matrix was noted. The solidification temperature exceeded the AZ31B melting temperature found in agglomerate particles reported by Thakur et al. [33].

Fig. 3(d) illustrates the surface morphology of NC3 composite containing 6 wt% of ZrO_2 nanoparticles. This microstructure showed a coarse aggregate structure with uniformly distributed particles. There were no casting defects and scratches due to improper

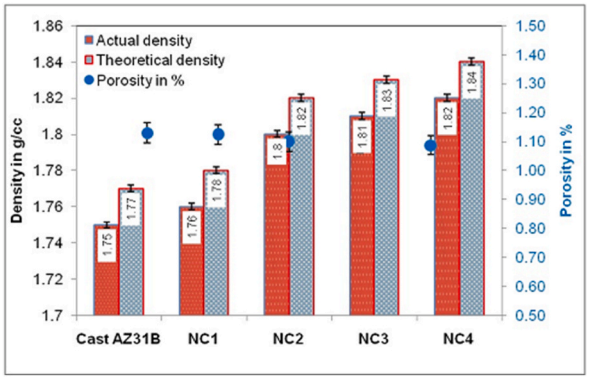

Fig. 2. Actual/theoretical density and percentages of porosity of developed AZ31B/ZrO_2 nanocomposite.

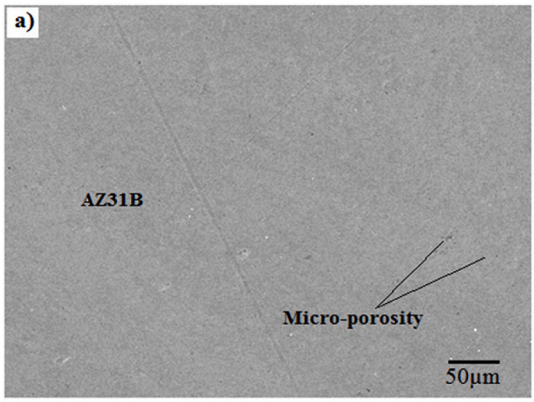

Fig. 3(a). Surface morphology of cast AZ31B alloy.

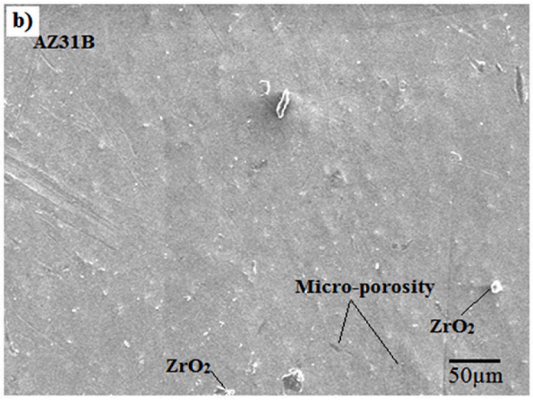

Fig. 3(b). Surface morphology of NC1.

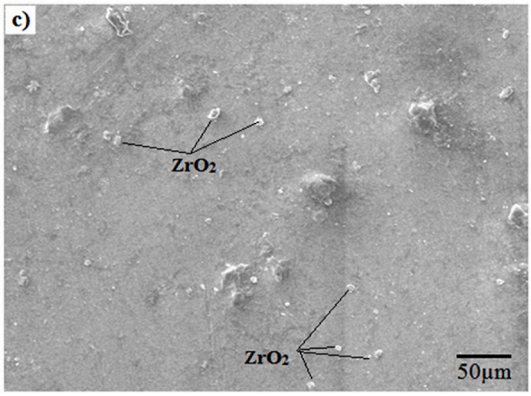

Fig. 3(c). Surface morphology of NC2.

polishing of test samples. However, the ZrO_2 presence in AZ31B alloy was proved, and its defect-free microstructure is shown in Fig. 3 (d).

The surface morphology of AZ31B alloy composite synthesized with ZrO_2 as 8 wt% is shown in Fig. 3(e). The reinforcements showed random distribution with agglomerated particle formation. This was due to the nature of the higher temperature above the melting temperature of the base matrix [22]. It changes to reduce the tensile strength of the composite [23,24]. However, the AZ31B alloy and its ZrO_2 filled nanocomposites proved their distribution along the AZ31B alloy matrix and showed a few agglomeration/microporosity. Based on the past literature, the optimum particle distribution was achieved, and its mechanical performances

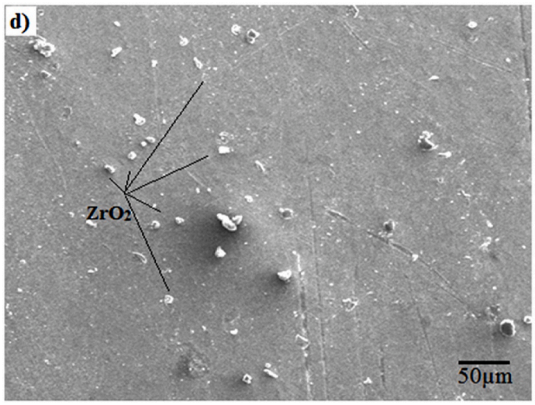

Fig. 3(d). Surface morphology of NC3.

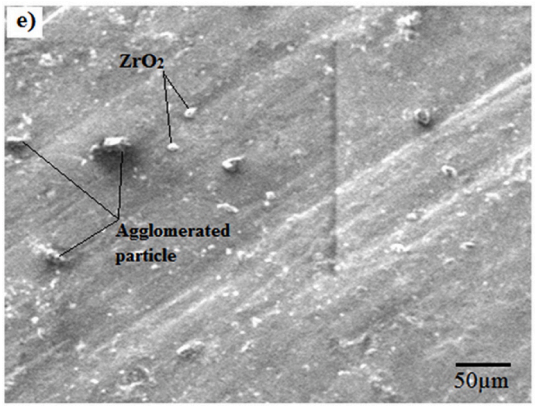

Fig. 3(e). Surface morphology of NC3.

are explained below.

3.3. Microhardness number

Here, the effect of resistance against the indentation for developed AZ31B alloy nanocomposite with and without ZrO_2 nanoparticle is shown in Fig. 4. Cast AZ31B alloy microhardness was 62.3 ± 1.1 HV and the inclusions of ZrO_2 as 2, 4, and 6 wt% recorded the significant improvement in hardness value compared to cast AZ31B alloy. Composite hardness was enhanced because ZrO_2 can withstand the maximum indentation load without failure [26]. The hard ceramic particle in a soft magnesium matrix has good hardness and tribological characteristics [7,10]. The composite contained maximum weight percentages of ZrO_2, proving their potential for a 25.68 % improvement in hardness. The mechanism for better pinning effect between the matrix and reinforcement was the reason for maximum hardness [18].

Moreover, the hardness of NC4 nanocomposite containing 8 wt% ZrO_2 was identified as the highest hardness (78.3 ± 1 HV) owing to homogenously distributed particles proved in Fig. 3(e). In addition, the choice of reinforcement and the selection of stir casting parameters was one factor deciding the hardness of the composite [24]. The maximum hardness of the NC4 sample compared with past reported values [25] showed a 6.5 % improvement in hardness. Previous reports of magnesium alloy (AZ31) composite synthesized with SiC recorded higher hardness values than cast AZ31 alloy [28].

3.4. Stress-strain behaviour

Here, the tensile behaviour of AZ31B alloy composite synthesized with 0, 2, 4, 6, and 8 wt% of ZrO_2 nanoparticle is shown in Fig. 5. During the evaluation, the stress-strain plot was generated via an electronic tool with various fields of yield, ultimate, and elongation. The details are represented in Table 5.

The stress-strain behaviour of cast AZ31B cast alloy was noted in Fig. 5. The yield strength and ultimate tensile strength of AZ31B cast alloy were 194 ± 4 MPa & 250 ± 3 MPa with elongation of 5.28 mm.

Generally, the AZ31B alloy has good tensile and deformation properties [2,10]. While the additions of 2 wt% ZrO_2 nanoparticle in

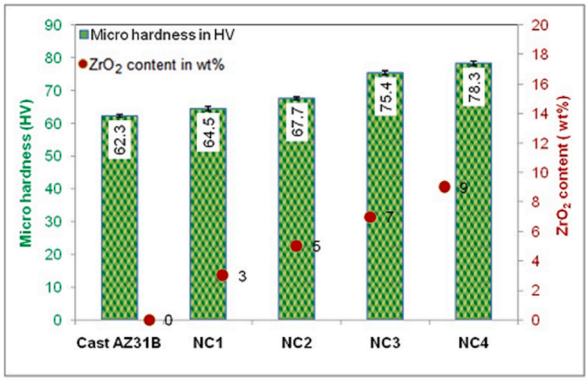

Fig. 4. Microhardness of developed AZ31B/ZrO_2 nanocomposites.

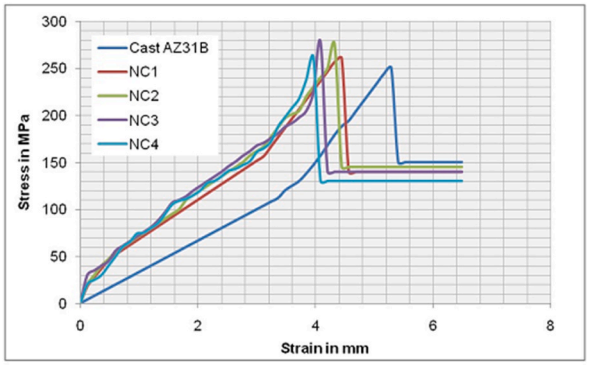

Fig. 5. Stress-strain curve for developed AZ31B/ZrO_2 nanocomposites.

Table 5
Tensile behaviour of AZ31B alloy nanocomposites.

S.No	Composite Identification	Strength in MPa		Rate of elongation
		Yield	Ultimate tensile	δ in mm
1	Cast AZ31B	194 ± 4	250 ± 3	5.28
2	NC1	201 ± 3	261 ± 5	4.44
3	NC2	209 ± 2	275 ± 3	4.32
4	NC3	212 ± 3	278 ± 2	4.08
5	NC4	202 ± 4	261 ± 4	3.96

AZ31B alloy found an increased yield strength (YS) & ultimate tensile strength (UTS)of 201 ± 3 MPa and 261 ± 5 MPa. The improvement in tensile strength of the composite was the reason for uniform particle distribution (Fig. 3(b)), with an effective bonding leading to withstand high tensile force. The interfacial bonding strength between the matrix and reinforcement offered maximum tensile strength before breaking the tensile specimen [14]. Moreover, further inclusions of ZrO_2 as 4 and 6 wt% showed superior tensile strength behaviour, and the ultimate strength of NC2 and NC3 was 275 ± 3 MPa and 278 ± 2 MPa, respectively. While compared to AZ31B cast alloy, the NC3 nanocomposite recorded the highest UTS and increased by 11.2 %. The composite enhancement was due to the solid strengthening mechanism between magnesium alloy and nano ZrO_2, which restricted particle movement's dislocation during high tensile force.

Moreover, the better adhesive nature between magnesium alloy and its reinforcement makes for better tensile strength [17]. Based on the content of reinforcements, the tensile strength was varied [18]. The maximum wt% of ZrO_2 nanoparticle in the matrix found decreased YS and UTS of 202 ± 4 and 261 ± 4 MPa. It was due to the microporosity inside the casting and agglomerated particle, evidenced in Fig. 3(e). It was due to the nature of reinforcement [20]. Generally, hard ceramic particles with maximum content offered high hardness results in decreased tensile strength [22].

However, the elongation performance of AZ31B alloy nanocomposite consists of 0, 2, 4, 6, and 8 wt% ZrO_2 showed marginal decrement. The deformation of cast AZ31B was 5.28 mm, while the inclusions of ZrO_2 as 2 wt% showed 4.44 mm. Similarly, increased ZrO_2 content has recorded increased tensile with decreased elongation rate due to the presence of ZrO_2 nanoparticles. It withstands the

maximum load before breaking a tensile specimen. Most of the research proved the significance of tensile strength by adding hard ceramic particles, and the ductility was limited [24–28].

3.5. Impact strength

The impact strength of developed AZ31 alloy with and without ZrO_2 nanoparticles is shown in Fig. 6. The impact strength of the nanocomposite was higher than that of casted magnesium alloy. The impact strength of composite without ZrO_2 was 13.1 ± 0.5 J/mm^2, and adding 2 and 4 wt% ZrO_2 in AZ31B alloy found progressive increment in impact strength and was 14 ± 0.3 and 15.9 ± 0.2 J/mm^2.

The enhancement of impact strength of nanocomposite was due to a better coupling effect between ZrO_2 nanoparticles and AZ31B alloy matrix. Baraniraj et al. [18] reported an effective interfacial strength between AZ31B/ZrO_2 leads to high impact strength. In addition, the nanocomposite containing 6 wt% of ZrO_2 recorded maximum impact strength and found a 25.19 % improvement compared to cast AZ31B alloy. During the maximum impact load, ZrO_2 resists and absorbs the maximum energy due to the higher pinning effect between ZrO2 and AZ31B alloy. Moreover, the impact strength of the nanocomposite was reduced to 15.5 ± 0.2 J/mm^2 on the maximum content of ZrO_2 as 8 wt%. It was due to agglomerated particle dislocation during the high-impact force.

Finally, present experimental outcome results were compared with past literature, as shown in Table 6. It was shown that the recent literature related to AZ31 magnesium alloy-based composite and ZrO_2 blended with aluminium alloy composite. Based on the availability of reported value for an existing system, the main key findings were compared and discussed below.

The results of AZ31B alloy nanocomposite developed with 6 wt% showed a 36 % improvement in yield strength compared to the reported value of composite prepared with AZ31/6 wt% TiC [12]. In addition, the ultimate tensile strength of nanocomposite found maximum value and increased by 17.7 %, 53.59 %, and 58.94 % as compared to the past reported value of AZ31/6 wt% TiC [12], AZ31/2 wt% alumina [23], and Al6061/6 wt% ZrO_2. While compared to past literature of Al6061/6 wt% ZrO_2 composite, the present composite hardness was improved by 11.2 %, and weight was saved by 57.45 %, respectively.

Based on this investigation, the higher content of ZrO_2, more than 6 wt%, limits the mechanical behaviour of nanocomposite. However, more than 6 wt% of ZrO_2 offered maximum microhardness value and was suitable for resistance against wear. So, future research plans to study the wear characteristics under different loads and speeds.

4. Conclusions

Here, the AZ31B alloy nanocomposite was made with 0, 2, 4, 6, and 8 wt% of ZrO_2 via liquid metallurgy stir cast method under argon nature. The applied uniform stir speed of 200 rpm proved their significance on AZ31B alloy nanocomposite, found uniform particle distribution with few agglomerated particles due to high solubility temperature more than the melting temperature of AZ31B alloy. Among the various combinations, the AZ31B alloy nanocomposite synthesized with 6 wt% (NC3) found superior hardness, yield strength, tensile strength and impact toughness, which was hiked by 21 %, 9.2 %, 11.2 %, and 25.19 % compared to casted AZ31B alloy. Moreover, the AZ31B alloy nanocomposite with 6 wt% recorded optimum experimental results compared with cast AZ31B alloy and past reported literature. According to this, it was suggested to lightweight to high-strength structural applications.

Funding statement

No funding was used for this study.

Data availability

All the data required are available within the manuscript.

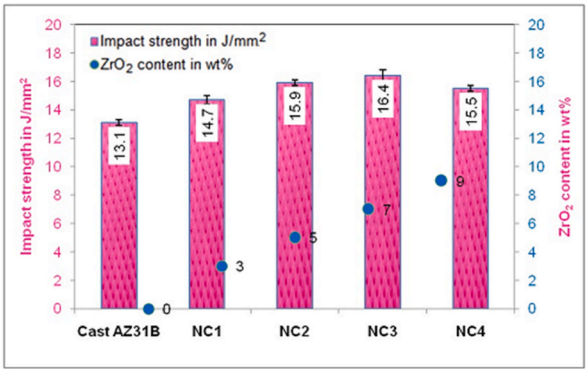

Fig. 6. Impact strength of developed AZ31B/ZrO_2 nanocomposites.

Table 6
Comparison of present results with past literature.

S.No	Composite details	Density	Yield strength	Tensile strength	Micro hardness	Reference
		g/cc	MPa	MPa	HV	
1	AZ31/1 wt% CNT	–	–	–	46	[3]
2	AZ31/10 vol% fly ash	1.79	–	–	62	[11]
3	AZ31/6 wt% TiC	–	155	236	108.2	[12]
4	AZ31/2 wt% Alumina	–	–	181	–	[23]
5	Al6061/6 wt% ZrO_2	2.85	–	174.9	67.8	[25]
6	AZ31B/6 wt% ZrO_2	1.81	212	278	75.4	Present work

CRediT authorship contribution statement

R. Venkatesh: Data curation, Conceptualization. **M. Vignesh Kumar:** Funding acquisition, Formal analysis. **I. Kantharaj:** Methodology, Investigation. **Roshita David:** Resources, Project administration. **Melvin Victor De Poures:** Supervision, Software. **Ismail Hossain:** Visualization, Validation. **A.H. Seikh:** Validation, Supervision. **M.A. Kalam:** Software, Resources. **Murugan P:** Writing – review & editing, Writing – original draft.

Declaration of competing interest

The authors declare that they have no known competing financial interests or personal relationships that could have appeared to influence the work reported in this paper.

Acknowledgements

The authors would like to acknowledge the Researchers Supporting Project number (RSP2024R373), King Saud University, Riyadh, Saudi Arabia. The research funding from the Ministry of Science and Higher Education of the Russian Federation (Ural Federal University Program of Development within the Priority-2030 Program) is gratefully acknowledged.

References

[1] S. Sudhagar, S. Sathees Kumar, V. Vijayan, R. Venkatesh, UV and Visible-light driven TiO_2/La_2O_3 and TiO_2/Al_2O_3 nanocatalysts: Synthesis and enhanced photocatalytic activity, Appl. Phys. A 128 (2022) 282, https://doi.org/10.1007/s00339-022-05293-7.
[2] C. Blawert, N. Hort, K. Kanier, Automotive application of magnesium and its alloys, Trans. Indian Inst. Met. 57 (2004) 397–408.
[3] A. Abbas, S.J. Huang, K. Sulleiova, Tribological effects of carbon nanotubes on magnesium alloy AZ31 and analyzing aging effects on CNTs/AZ31 composites fabricated by stir casting process, Tribol. Int. 142 (2020) 105982, https://doi.org/10.1016/j.triboint.2019.105982.
[4] A. Baraniraj, A.P. Sathiyagananam, Ra Aravind, Silicon carbide particle Enriched magnesium alloy (AZ91) composite: physical, microstructural and mechanical studies, Silicon (2023), https://doi.org/10.1007/s12633-023-02516-1.
[5] T. Thirugnanasambandham, J. Chandradass, L.J. Martin, Fabrication and mechanical properties of alumina nanoparticle reinforced magnesium metal matrix composite by stir casting method, SAE Technical paper 2018-28-0098 (2018), https://doi.org/10.4271/2018-28-0098.
[6] S. Ravichandran, R. Duraiswamy, F.S. Arockiasamy, Tool and formability multi-response optimization for ultimate strength and ductility of AA8011 during axial compression, Adv. Mech. Eng. 14 (10) (2022) 1–12, https://doi.org/10.1177/16878132221131731.
[7] S.V. Prasad, R. Asthana, Aluminum metal-matrix composites for automotive applications: tribological considerations, Tribology letter 17 (2004) 445–453, https://doi.org/10.1023/B:TRIL.0000044492.91991.f3.
[8] B.A. Kumar, M.M. Krishnan, H.L. Allasi, Characterization of the aluminium matrix composite reinforced with silicon nitride (AA6061/Si3N4) synthesized by the stir casting route, Adv. Mater. Sci. Eng. (2022), https://doi.org/10.1155/2022/8761865. Aritle ID 8761865.
[9] C. Ramesh Kannan, R. Venkatesh, M. Vivekanandan, Synthesis and characterization of mechanical properties of AA8014 + Si3N4/ZrO2 hybrid composites by stir casting process, Journal of Advances in Materials Science and Engineering 2022 (2022) 11. Article ID 9150442.
[10] B.L. Mordike, T. Ebert, "Magnesium: properties, applications, and potential, Mater. Sci. Eng. A 302 (2001) 37–45, https://doi.org/10.1016/S0921-5093(00)01351-4.
[11] I. Dinaharan, S.C. Vettivel, E.T. Akinlabi, Influence of processing route on microstructure and wear resistance of fly ash reinforced AZ31 magnesium matrix composites, J. Magnes. Alloy 7 (1) (2019) 155–165, https://doi.org/10.1016/j.jma.2019.01.003.
[12] G. Kaliyaperumal, S. Elango, M.V.D. Poures, Experimental study and TiC interfacial action on microstructural and mechanical properties of AZ31 alloy composite made by stir casting route, Mater.Today: Proc. (2023), https://doi.org/10.1016/j.matpr.2023.06.131.
[13] J. Zhou, L. Ren, H. Hu, As-cast magnesium AM60-based hybrid nanocomposite containing alumina fibres and nanoparticles: microstructure and tensile behaviour, Material science and engineering: A 740–741 (2019) 305–314, https://doi.org/10.1016/j.msea.2017.10.070.
[14] B. Ratna Sunil, G. Pradeep Kumar Reddy, H. Patle, R. Dumpala, Magnesium based surface metal matrix composites by friction stir processing, J. Magnesium Alloys 4 (2016) 52–61, https://doi.org/10.1016/2016-02-001, 2016.
[15] M. Rashad, F. Pan, M. Asif, A. Ullah, "Improved mechanical properties of magnesium based composites with titanium—aluminium hybrids, J. Magnesium Alloys 3 (1) (2015) 1–9, https://doi.org/10.1016/2014-12-010, 2015.
[16] C.L. Zhang, X.J. Wang, K. Wu, 2016)"Fabrication, microstructure and mechanical properties of Mg matrix composites reinforced by high volume fraction of sphere TC4 particles, J. Magnesium Alloys 4 (4) (2016) 286–294, https://doi.org/10.1016/2016-10-003.
[17] J. Chandradass, T. Thirugnanasambandham, P.B. Sethupathi, Liquid state stir cast processing and characteristics study of AZ91D/SiCp composites, Mater.Today: Proc. 45 (7) (2021) 6507–6511, https://doi.org/10.1016/j.matpr.2020.11.450.
[18] A. Baraniraj, A.P. Sathiyagnanam, M.V. Pources, Vacuum stir cast developed aluminium alloy hybrid nanocomposite performance compared with gravity cast: mechanical and tribological characteristics study, Inter Metalcast (2023), https://doi.org/10.1007/s40962-023-01119-1.
[19] S. Tanoue, H. Uematsu, Characterization of polypropylene/magnesium oxide/vapour-grown carbon fiber composites prepared by melt compounding, J. Polym. Eng. 42 (3) (2021) 204–213, https://doi.org/10.1515/polyeng-2021-0201.

[20] D. Sameer Kumar, K.N.S. Suman, S.B. Venkata Siva, "Microstructure, mechanical response and fractography of AZ91E/Al_2O_3 (P) nanocomposite fabricated by semisolid stir casting method", 2017, J. Magnesium Alloys 5 (1) (2017) 48–55, https://doi.org/10.1016/2016-11-006.
[21] D. Kumar, R.K. Phanden, L. Thakur, A review on environment-friendly and lightweight magnesium based metal matrix composites and alloys, Mater. Today Proc. 38 (1) (2021) 359–364, https://doi.org/10.1016/j.matpr.2020.07.424.
[22] M.J. Shen, X.J. Wang, K. Wu, Microstructure and room temperature tensile properties of 1lm-SiCp/AZ31B magnesium matrix composite, J. Magnesium Alloys 3 (2015) 155–161, https://doi.org/10.1016/2015-03-001.
[23] A. Khandelwai, K. Mani, G.P. Chaudhari, Mechanical behaviour of AZ31/Al_2O_3 magnesium alloy nanocomposites prepared using ultrasound assisted stir casting, Compos. B Eng. 123 (2017) 64–73, https://doi.org/10.1016/j.compositesb.2017.05.007.
[24] S. Banerjee, S. Poria, P. Sahoo, Ry sliding tribological behaviour of AZ31-WC nanocomposite, J. Magnesium Alloys 7 (2) (2019) 315–327, https://doi.org/10.1016/j.jma.2018.11.005.
[25] G.B. Veeresh Kumar, R. Pramod, T. Bhanumurthy, Investigation of physical, mechanical and tribological properties of Al6061–ZrO_2 nanocomposite, Heliyon 5 (2019) e02858, https://doi.org/10.1016/j.heliyon.2019.e02858.
[26] M. Rajkumar, N. Senthil Kannan, Subbiah Ram, Cryogenic treatment and taguchi optimization of Haynes allo, Mater. Today Proc. 51 (1) (2021) 666–669, https://doi.org/10.1016/j.matpr.2021.06.159.
[27] S.J. Huang, M. Subramani, C.C. Chiang, Effect of hybrid reinforcement on microstructure and mechanical properties of AZ61 magnesium alloy processed by stir casting method, Composite communications 25 (2021) 100772, https://doi.org/10.1016/j.coco.2021.100772.
[28] K.C.K. Kumar, B.R. Kumar, N. Mohan, Microstructural, mechanical characterization, and fractography of AZ31/SiC reinforced composites by stir casting metho, Silicon 1 (2022) 5017–5027, https://doi.org/10.1007/s12633-021-01180-7.
[29] S.U.I. Sheikh, N.M. Khan, M.M. Khan, Effect of reinforcement on magnesium-based composites fabricated through stir casting: a review, Mater. Today Proc. 46 (15) (2021) 6513–6518, https://doi.org/10.1016/j.matpr.2021.03.710.
[30] G. Ma, H. Xiao, Y. He, Research status and development of magnesium matrix composite, Material Sci. Technol. (2020) 645–653, https://doi.org/10.1080/02670836.2020.1732610.
[31] Hanizam, H., Salleh, M.S "n of carbon nanotubes–aluminium alloy composite through Taguchi method" J. Mater. Res. Technol. 8(2), 2223-2231. https://doi.org/10.1016/j.jmrt.2019.02.008..
[32] R. Venkatesh, S. Siva Chandran, 'Magnesium alloy machining and its methodology: a systematic review and analyses, AIP Conf. Proc. 2473 (1) (2022), https://doi.org/10.1063/5.0096398.
[33] B. Thakur, S. Barve, P. Pesode, Investigation on mechanical properties of AZ31B magnesium alloy manufactured by stir casting process, J. Mech. Behav. Biomed. Mater. 138 (2023) 105641, https://doi.org/10.1016/j.jmbbm.2022.105641.
[34] A. Sobhanadri, G. Senthilkumar, M. Vivekanandan, A CFD investigation and heat transfer augmentation of double pipe heat exchanger by employing helical baffles on shell and tube side, Therm. Sci. 26 (2A) (2022) 991–998.
[35] R. Venkatesh, P. Sakthivel, G. Selvakumar, et al., Mechanical and thermal properties of a waste fly ash-bonded Al-10 Mg alloy composite improved by bioceramic silicon nanoparticles, Biomass Conv. Bioref. (2023), https://doi.org/10.1007/s13399-023-04588-w.
[36] R. Venkatesh, M.K.V. Karthikeyan, R. Sasikumar, et al., Effective utilization of silica from waste cow dung ash filler reinforced biodegradable jute epoxy composites: influence of silica on its mechanical properties, Biomass Conv. Bioref. (2023), https://doi.org/10.1007/s13399-023-04505-1.
[37] G.A.C. Jayaseelan, A. Surenderpaul, T.T. Selvam, et al., Assessment of solar thermal monitoring of heat pump by using zeolite, silica gel, and alumina nanofluid, Clean Technol. Environ. Policy (2023), https://doi.org/10.1007/s10098-023-02558-4.
[38] N. Poyyamozhi, A. Sivanantham, N. Mukilarasan, K. Gopal, et al., Ecosystem sustainability and conservation of waste natural fiber strengthen epoxy composites for lightweight applications, Environ. Qual. Manag. 1–6 (2023), https://doi.org/10.1002/tqem.22047.
[39] J.S.N. Raju, M.V. Depoures, J. Shariff, S. Chakravarthy, et al., Characterization of natural cellulosic fibers from stem of symphirema involucratum plant, J. Nat. Fibers 19 (2022) 13, https://doi.org/10.1080/15440478.2021.1875376.